

## **Comparison of Storm Longshore Transport Rates to Predictions**

Herman C. Miller<sup>1</sup>, M ASCE

### Abstract

Longshore sediment transport (LST) is of primary importance to long-term shoreline changes and must be accounted for in most coastal designs. Predicting LST has been hampered by the lack of direct measurements during storm conditions against which the models can be calibrated. The Sensor Insertion System (SIS) developed at the US Army Corps of Engineers (USACE) Field Research Facility provides a way to directly measure LST during storms. The SIS was operated during the growth, peak, and waning stages of three storms between April, 1997 and February, 1998 in which the waves reached a maximum individual height of 5.6m. In up to 14 cross-shore locations, concentration and velocity measurements were made throughout the water column. These measurements were compared to total transport models of USACE 1984, Kamphius 1991, Kraus, et al. 1988, Walton 1980, and the cross-shore distribution model of Bodge and Dean 1987. The results show the storm measurements had a consistent pattern; rapidly increasing to a peak rate, then gradually decreasing during the waning stages of each storm. Cross-shore distributions of longshore flux tended to peak over the offshore bar and at the beach where wave dissipation caused high suspended sediment concentrations. These peaks were not co-located with maximum longshore currents, which tended to peak at mid-surf. The comparisons show that the models would benefit from comparison to the storm measurements.

### Introduction

Anticipating long-term shoreline changes; designing coastal structures and beach renourishment projects; determining funding allocations for the maintenance of our navigable waterways, inlets, and harbors are some of the reasons it is important to predict longshore sediment transport (LST). Accurate predictions of LST has been a goal of coastal

---

<sup>1</sup>US Army Engineer Waterways Experiment Station Coastal & Hydraulics Laboratory Field Research Facility, 1261 Duck Road, Kitty Hawk, NC 27949, USA

engineers for decades. While many models have been introduced, some very sophisticated, others simple and robust, few have attained wide use (see reviews, Bodge 1989, Sternberg et al. 1989, Komar 1990, Kraus and Horikowa 1990). Consequently, the need for improvement continues. Until new models, based on a better understanding of the transport mechanisms are developed, improving the modeling capability might best be achieved by comparing existing models to field measurements during storms. It is well known that storms, with waves generally higher than 2 m, are responsible for the largest changes in our coasts. Thus, the models need to work well under these conditions. The problem is there is a paucity of these data. A thorough review of the LST data by Schoonees and Theron (1993) concluded that almost all field data were for wave heights below 1.8 m. The consequence is that existing transport models are calibrated against rates measured during low to moderate wave conditions.

This study has produced a number of high quality storm data sets. LST rates and highly-resolved cross-shore distributions of longshore sediment flux during three storms are compared to five easy to use LST formulations. The results demonstrate how LST models could benefit from field measurements under storm conditions. The paper includes brief descriptions of the site characteristics, a new system for making direct measurements during storms, instrumentation, and data collection/analysis procedures. Then, examples of the measurements are given and comparisons are made to LST models.

### Site Characteristics

This investigation was conducted in the United States (US) at the US Army Engineer Waterways Experiment Station, Coastal and Hydraulics Laboratory's Field Research Facility (FRF) located in Duck, North Carolina (NC), on the Atlantic Ocean (Figure 1). With an average of 20 storms per year, including the close passage of tropical storms and hurricanes, this site is ideal for studying sediment transport during storms.

The characteristics of the FRF have been well studied and the processes are summarized in the series of annual reports, (Leffler et al. 1998). Average annual significant wave height is near 1 m with a 9-sec period. Significant wave heights in excess of 4 m (in 8 m depth) are not uncommon. The tide is semi-diurnal tide with a spring range of 1.2 m and storm surges in excess of 1 m have been recorded. Wave information used in this study were collected from the FRF directional array located in 8 m depth (Long and Oltman-Shay 1991).

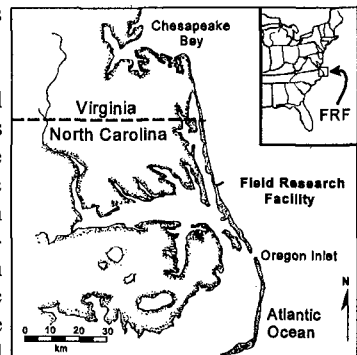


Figure 1. FRF Site

The beach, locally oriented NNW-SSE, is typical of the barrier island system along the mid-Atlantic coast of the US. The typical nearshore profile has two bars, but varies with season and longer time scales (Birkemeier 1984). The nearshore consists of 0.15 to

0.18 mm sand that grades toward 0.12 mm further offshore, with coarse sand and gravel from submerged river beds abundant at the beach (Stauble 1992, Schwartz et al. 1997).

Sensor Insertion System



Figure 2. SIS During October, 1997 Storm

There are many reasons for the lack of direct measurements of LST during storms, including the expense and logistics required to operate a monitoring program that can operate in severe wave conditions through many storms. To overcome this, the FRF has developed the Sensor Insertion System (SIS). The pier based SIS, Figure 2, is capable of measuring hydrodynamic processes and the resulting sediment transport anywhere across 500 m of the nearshore.

The SIS is a 70,000 kg crane with an array of instrumentation that is moved along the length of the research pier to measure sediment transport at different positions across the surf zone during storms. The SIS is designed to operate in up to 5.6-m individual wave heights. To minimize the influence of the pier, the SIS, with 20-m-long booms, can place instruments on the ocean bottom in 9 m depth as far as 22 m updrift of the pier centerline. This system provides an economical way to make these measurements. It does not require divers and can reposition the sensors as the profile evolves during a storm. A disadvantage of the SIS measurement system is that measurements across the shore are not simultaneous, but occur over a 3-hour period.

Instrumentation

Optical backscattering concentration sensors (OBS) in combination with electromagnetic current meters (EMCMs) have proven most reliable during storms for measuring sediment flux throughout the water column. Each concentration sensor is considered representative of a portion of the water column as shown in Figure 3. Many of

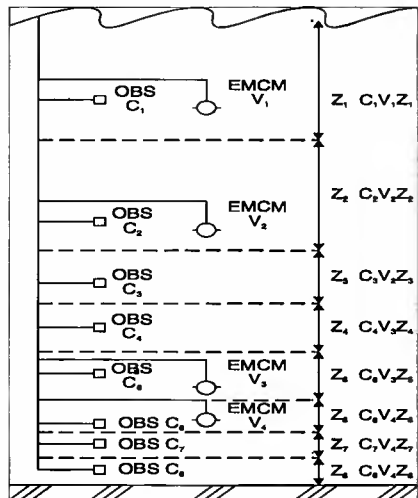


Figure 3. Schematic of SIS Flux Sensors

the sensors are positioned near the bottom since the measurements show that much of the sediment is transported within 1 m of the bed. The lowest concentration sensor is typically 3 to 5 cm above the bottom. Distance to the bottom is measured with a down-looking sonic altimeter.

The instruments are held updrift of the SIS on a frame as shown in Figure 4. This minimizes contamination of the measurements by any wake effect off the SIS. Since the instrumentation is parked on the pier deck between use, the instruments can be frequently inspected, rinsed with fresh water, are virtually unaffected by biological fouling, and thus tend to hold their calibrations well.



Figure 4. Sensors on SIS

### Data Collection And Analysis

This single instrument array was used to directly measure sediment concentration and fluid velocity at a large number of cross-shore locations. From these measurements the cross-shore flux distribution can be determined and integrated to compute the LST rate. Starting about 1½ hrs before high or low tide, and operating for 3 hours, up to 14 cross-shore locations can be measured while the water level changes very little. This provides a quasi-synoptic “snap-shot” of the cross-shore distribution of the longshore sediment flux. At each location along the pier, 512-sec-long records were sampled at 16 Hz. The high sample frequency is required because sand resuspension events last for only a fraction of the wave cycle. All of the cross-shore measurement locations along the pier during one tide will be referred to as a “transect.”

Instantaneous concentration and velocity values are used to compute the flux at each gauge location in the water column by multiplying the instantaneous concentration,  $c(x,z,t_i)$ , after accounting for the “turbidity” offset (Ludwig and Hanes 1990, Schoelhamer 1993), by the instantaneous longshore velocity,  $v(x,z,t_i)$ , and time-averaging the products.

$$F(x,z) = \frac{1}{N} \sum_{i=1}^N c(x,z,t_i) v(x,z,t_i) \quad (1)$$

where  $N$  is the number of samples and  $F(x,z)$  is the longshore sediment flux, which is the rate per unit area in the  $x$  (cross-shore) and  $z$  (vertical) directions.

Cross-shore distribution of the longshore flux was obtained by summing the vertical contributions at each location along the transect

$$G(x) = \sum_{j=1}^M F(x, z_j) \delta z_j \quad (2)$$

where  $G(x)$  is the vertically integrated flux per unit cross-shore length and  $M$  is the number of concentration sensors.

Longshore transport rates were computed in a similar way by summing the across-shore contributions

$$I = \sum_{k=1}^L G(x_k) \delta x_k \quad (3)$$

where  $L$  is the number of measurement locations and  $I$  is the longshore sediment transport rate. These rates were converted to volume transport rates,  $Q$  ( $\text{m}^3/\text{hr}$ ), assuming the density of quartz sand is  $2,650 \text{ kg/m}^3$ , the density of sea water is  $1,025 \text{ kg/m}^3$ , and the solid fraction is 0.6.

## Results

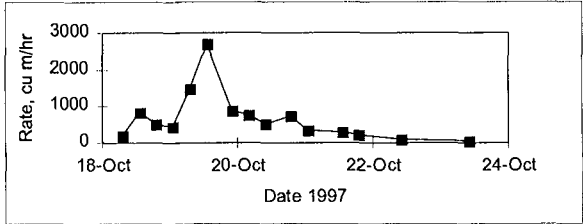
### Measured Transport Rates

Three storms were selected for analysis because the measurements included the growth, peak, and waning storm stages. The peak rates are compared in Table 1. With approximately the same peak wave directions and periods, the measured LST was observed to vary approximately linearly with wave energy up to a rate of  $3,400 \text{ m}^3/\text{hr}$ , the highest measured to date.

Table 1. Peak Transport Rates				
Date	Wave Height, m	Wave Period, sec	Wave Angle From Normal, Deg	Longshore Transport Rate, cu m/hr
1 Apr 97	2.7	9	18	1,500
19 Oct 97	3.3	10	20	2,700
4 Feb 98	3.8	11	20	3,400

The LST rates for each transect during the growth, peak, and waning stages of the October, 1997 storm are shown in Figure 5. The rapid growth to a peak, followed by a

gradual waning of the LST is typical of the storm measurements at the FRF. On 19 October, a total volume of 33,200 m<sup>3</sup> of sediment was measured moving south.



Cross-Shore Distribution

Figure 5. LST Rates During October, 1997 Storm

The unique capabilities of the SIS to rapidly reposition the sensors during a storm resulted in highly-resolved cross-shore distributions of longshore flux measurements. Cross-shore locations were selected to document both the peak and minimum values, so an

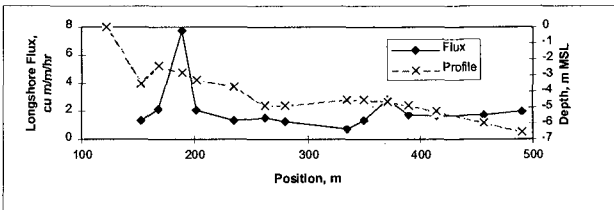


Figure 6. Flux Distribution, 20 Oct 97

of the longshore sediment flux with 14 measurement positions is shown in Figure 6. The graph is for one transect on 20 October, 1997 during low tide when the waves were 2.4 m. This example was chosen because it is a typical storm distribution.

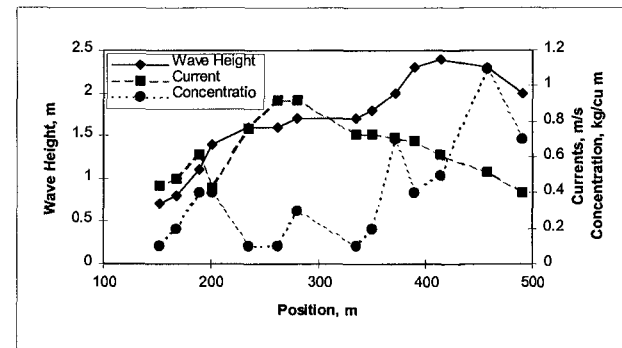


Figure 7. Processes Distribution, 20 October, 1997

processes. In Figure 7, wave height, longshore current from the near surface EMC, and near-bed sediment concentrations are displayed. Beginning offshore, the waves shoal and dissipate energy over the outer bar, remain consistent across the trough between the bars, before dissipating energy again at the inner bar and beach. The break point defining the surf

accurate representation of the LST rate could be determined. From experience obtained during many prior storm tests, a minimum of 8 cross-shore positions are required across the barred profile. An example of a cross-shore distribution of the longshore sediment flux per unit cross-shore length and water depth at the measurement locations. As can be seen, peak flux values are associated with the inner and outer bars along the profile.

It is interesting to compare the resulting flux values to the cross-shore distribution of the

zone would be considered located near position 425 m where predominate breaking occurred; however, breaking of the highest waves was observed seaward of that location. The longshore current builds to a peak over the trough between the bars. This distribution is somewhat like the classic longshore current distribution of Longuet-Higgins (1970) and has been observed previously at the FRF (Smith et al. 1993). Sediment concentration peaks are associated with wave shoaling and wave energy dissipation.

Comparing Figure 6 to 7 shows that the longshore sediment flux and sediment concentration peak at the same locations, which do not coincide with the longshore current peaks. The importance of wave dissipation suspending sediment in the cross-shore distribution of longshore flux is well documented in all of the storms measured to date. That is not to say this is the only cross-shore distribution of longshore flux. In fact, many different distributions have been measured that reflect differences in profile features and wave energy levels. For example, during low wave conditions, a single peak near the inshore bar or beach occurs.

### Comparison to LST Rate Models

Arguably, the most widely used LST model is that given in the Shore Protection Manual (SPM) (USACE 1984). This formulation equates,  $I$ , the immersed weight transport rate to a constant,  $K$ , times the longshore wave energy flux factor,  $P_{lb}$

$$I = K P_{lb} \quad (4)$$

where  $K$  equals 0.39 when using significant wave height. This constant was determined primarily from long-term averaging of waves and sediment accumulation at coastal structures.

The longshore wave energy flux factor is given in terms of the wave conditions at breaking

$$P_{lb} = (E C_g)_b \sin \alpha_b \cos \alpha_b \quad (5)$$

where  $E$  is the wave energy,  $C_g$  is the wave group velocity,  $\alpha$  is the wave crest angle relative to the beach, and "b" denotes breaking conditions.

For these predictions, the peak wave parameters measured at the FRF's directional array were shoaled conserving wave energy flux according to

$$E_{d.a.} C_{gd.a.} \cos \alpha_{d.a.} = E_b C_{gb} \cos \alpha_b \quad (6)$$

and the waves were refracted using Snell's Law:

$$\frac{\sin \alpha_{d.a.}}{L_{d.a.}} = \frac{\sin \alpha_b}{L_b} \tag{7}$$

where L is the wave length and "d.a." is at the directional array. A breaking criteria of H/d = 0.78 was used.

The SPM predictions were made every 3 hrs when the wave data were available. The LST measurements are only at times of high or low tide. Figure 8 compares the measured and predicted LST rates. In this case, the SPM somewhat overpredicted the lower rates and underpredicted the peak rate. However, in general, it compared reasonably well with the measurements. Note, after more storm measurements are obtained and an error analysis is performed, many of these differences may prove insignificant.

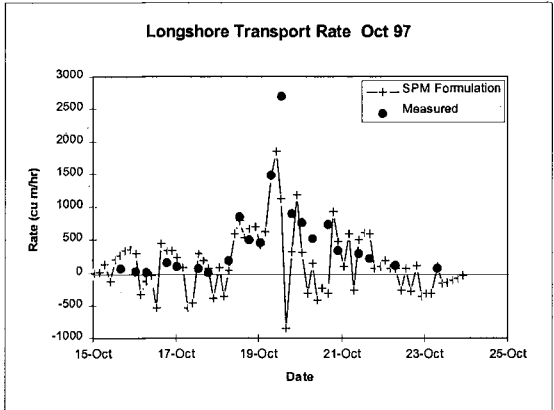


Figure 8. SPM Predictions and Measurements; Oct 97

The SPM predictions show a high degree of variability. This is in part because the SPM assumes all the wave energy is in a single wave train. Because the storms tend to move along the coast past the FRF, multiple peaked spectra frequently are measured. Small shifts in the energy level of similar spectral peaks can cause considerable variation from one prediction to the next.

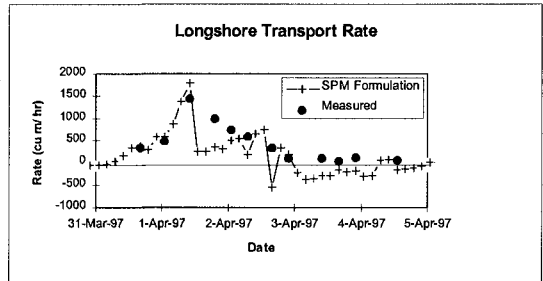


Figure 9. SPM Predictions and Measurements; Apr 97

Figure 9 shows a similar comparison between SPM predictions and measurements for the storm in April, 1997. Again there is reasonable agreement, particularly, during the growth and peak of the storm; although, in this case the peak was over predicted. The measured LST gradually decreased as is common during the waning stages of the storm.

Negative predictions indicate a direction reversal caused by the arrival of the southerly swell after the storm passed.

For the February, 1998 storm (Figure 10) the waves were from the south side of the pier and the transport was directed to the north as designated by the negative values. The SPM formulation over predicted the peak.

The Kamphius 1991 model was attractive because it included bottom slope, sediment size, and wave period, in addition to the wave height and angle of approach.

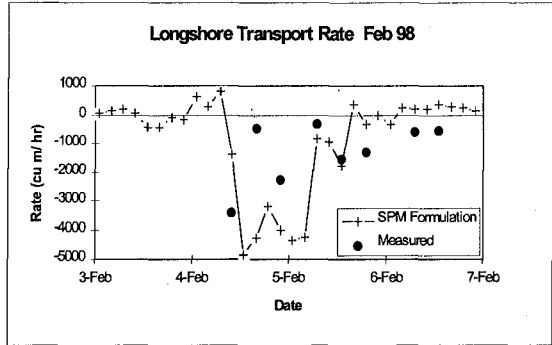


Figure 10. SPM Predictions and Measurements; Feb 98

$$Q = 7.3 H_{sb}^2 T_p^{1.5} m_b^{0.75} D_{50}^{-0.25} \sin^{0.6}(2\alpha_b) \tag{8}$$

where  $H_{sb}$  is the significant wave height at breaking,  $T_p$  is the peak spectral wave period,  $m_b$  is the bottom slope,  $D_{50}$  is the sediment size, and  $\alpha_b$  is the wave angle at breaking.

Using the transects near the peak of the April, 1997 storm, Figure 11, shows the model underpredicts the magnitude of the rates. The Kamphius coefficient was evaluated primarily with laboratory data. It appears the predictions are off by an order of magnitude. When the Kamphius coefficient is multiplied by a factor of 10, Figure 12, the predictions are improved.

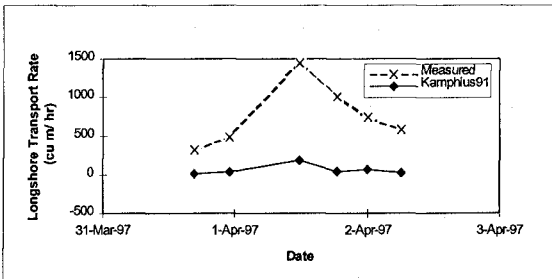


Figure 11. Kamphius Predictions, April, 1997 Storm

Kraus et al. (1988) proposed a LST rate model which included a water discharge parameter,  $R$ , which must exceed a critical discharge value they call  $R_c$ ,

$$I = 2.7 (R - R_c) \tag{9}$$

where the discharge parameter,  $R$ , is

$$R = V X_b H_{sb} \tag{10}$$

with  $V$  the longshore velocity,  $X_b$  the surf zone width,  $H_{sb}$  the significant wave height, and  $R_c = 3.9 \text{ m}^3 / \text{sec}$ .

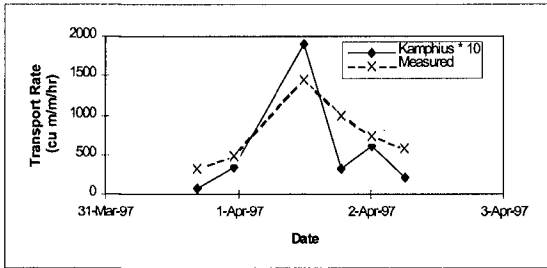


Figure 12. Modified Kamphius Predictions

This model, which was developed from field measurements under low to moderate wave conditions, is compared to three transects during the April, 1997 storm (Table 2). These transects were chosen because of the range of wave heights. The model underpredicts the measured values from 30 to 60 percent.

Kraus et al. (1988) provide a velocity term correction based on the standard deviation of the velocity and another correction based on the wave height gradient, but these did not improve the results. This model, which is easily applied, may only lack the storm measurements to recalibrate the model coefficient.

Transect	$H_{sb}$ , m	$V$ , m/s	$X$ , m	$Q_{pred}$ , $\text{m}^3/\text{hr}$	$Q_{meas}$ , $\text{m}^3/\text{hr}$	$Q_{pred} / Q_{meas}$
2	1.6	0.49	220	170	480	0.4
6	2.5	1.18	198	610	740	0.8
4	3.0	1.21	300	1100	1500	0.7

The Walton (1980) model was intriguing because it included Longuet-Higgins cross-shore current distribution and a water discharge parameter that resembled that of Kraus et al. (1988).

$$P_{ls} = \rho g \frac{H_{sb} W V C_f}{\frac{5\pi}{2} \left(\frac{v}{v_o}\right)_{LH}} \tag{11}$$

where W is the surf zone width, C<sub>f</sub> is a friction coefficient and the Longuet-Higgins current distribution is given by

$$\left(\frac{V}{V_o}\right)_{LH} = 0.2 \left(\frac{X}{W}\right) - 0.74 \left(\frac{X}{W}\right) \ln\left(\frac{X}{W}\right) \tag{12}$$

with X being the cross-shore position that the velocity was measured.

For the same three transects, the Walton model greatly overpredicts the LST rate (Table 3). However, there is some similarity in how the Walton and Kraus et al. models differed from the measurements. The prediction to measurement factor, Q<sub>p</sub>/Q<sub>m</sub>, for transects 4 and 6 are about twice that for transect 2 for both models. The similarity in how the models perform is probably because both models have a water discharge parameter. Recalibration with data from multiple storms should benefit these models.

Table 3. Walton, 1980 Predictions for April, 1997 Storm							
Transect	H <sub>sb</sub> , m	V, m/s	X, m	W, m	Q <sub>pred</sub> , m <sup>3</sup> /hr	Q <sub>meas</sub> , m <sup>3</sup> /hr	Q <sub>pred</sub> / Q <sub>meas</sub>
2	1.6	0.49	220	22	910	480	1.9
6	2.5	1.18	198	198	3100	740	4.2
4	3.0	1.21	300	300	8100	1500	5.4

Comparison to Cross-Shore Distribution Models

The new USACE Coastal Engineering Manual (CEM) (scheduled for publication and public release in 2000) presents the cross-shore distribution of longshore sediment flux proposed by Bodge & Dean (1987) as an example of the available models. This model is attractive because it includes wave energy dissipation and longshore velocity and therefore

can account for local wind effects and depth.

$$q_x(y) = \frac{k_q}{d} \frac{\delta}{\delta x} (E C_g) V_l \tag{13}$$

The dimensional constant,  $k_q = 48$  sec, was evaluated from laboratory experiments and low to moderate wave conditions in the field. As can be seen in Figure 13, the model re-creates the peaks over the bars for this transect near the peak of the storm. It is interesting to note that the strong dependence of the model on wave dissipation resulted in negative predictions, (that do not represent a direction reversal), at the seaward most locations where the waves were shoaling.

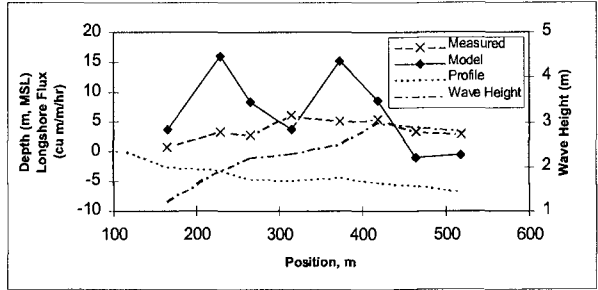


Figure 13. Bodge and Dean Predictions, 1 April, 1997

Bodge & Dean (1987) indicate the model is only valid inside the surf zone where the wave energy is expected to dissipate. The magnitudes of the predictions appear to be much larger than the measured flux values. Bodge and Dean do provide a correction that is dependent on the bottom slope; however, that made the agreement worse. Since it appears from matching the first few

values in Figure 13 that the predictions are approximately a factor of four larger than the measurements,  $k_q$  was reduced to 0.12 sec and replotted in Figure 14. The agreement, although not perfect, is better. The intent here is not a rigorous recalibration of the models, but simply a first attempt to demonstrate the utility of the measurements. After more measurements are obtained,

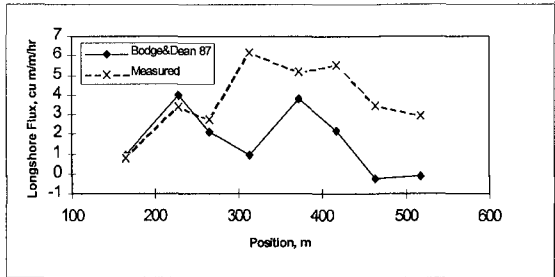


Figure 14. Modified Bodge and Dean Predictions

model recalibrations will be performed. The goal of the SIS measurement program is to gather data during storms so models, such as this, can be calibrated under a range of storm wave conditions and improve our ability to predict LST. Two other distribution models (Briand and Kamphius 1993, Watanabe, et al. 1991) were considered, but proved difficult to apply.

## Conclusions

The SIS provides a powerful platform to measure LST during storms. Quasi-synoptic "snap shots" of highly-resolved cross-shore distributions of longshore flux have been obtained for storms with significant wave heights that reached 3.8 m. LST rates as high as 3,400 m<sup>3</sup> per hour were measured. For the three storms presented, the transport rate rapidly increased to a peak, then gradually decreased during the waning stages of the storms.

The cross-shore distribution of longshore sediment flux shows that, near the peak of a storm, maxima occur over the bars where the wave dissipation increases the suspended-sediment concentration. These, in general, are not co-located with the longshore current maxima which tends to peak over the trough between the bars.

The SPM formulation seemed to capture the trend of the measurements reasonably well. The SPM tends to over predict low wave conditions. The SPM shows considerable variability, even direction reversals, during the waning stages of a storm. This was due to the presence of sea and swell with comparable energy levels due to the rapidly moving storm systems which are common at the FRF. The Kraus et al. (1988) model underpredicted the LST rates. Walton (1980) over predicted the rates. These models would benefit from comparison to storm measurements.

The shape of the cross-shore distribution of longshore sediment flux was modeled reasonably well in the surf zone by Bodge and Dean (1987). Their wave energy dissipation model overpredicted the magnitude. Reducing their coefficient by a factor of four improved the agreement.

While this investigation is a start toward filling the need for storm measurements that can be used to calibrate existing models and develop improved formulations, additional measurements over a range of conditions are still needed and will be a future focus.

## References

- Birkemeier, W. A. (1984). "Time scales of nearshore profile changes," Proc. 19<sup>th</sup> Coastal Eng. Conf., Houston, Texas, ASCE, 1507-1521.
- Bodge, K.R. (1989). "A literature review of the distribution of longshore sediment transport across the surf zone," J. Coastal Res., Vol 5, No 2, 307-328.
- Bodge, K. R., and Dean, R. G. (1987). "Short-Term Impoundment of Longshore Sediment Transport," TR CERC-87-7, WES, Vicksburg, Miss.
- Briand, M. G. and Kamphuis, J.W. (1993). "Sediment transport in the surf zone: a quasi 3-D numerical model," Coastal Eng., Vol 20, 135-156.
- Kamphuis, J.W. (1991). "Alongshore sediment transport rate," J. of Waterway, Port, Coastal, and Ocean Eng., ASCE, Vol. 117, No. 6, 624-640.
- Komar, P.D. (1990). "Littoral sediment transport," In Handbook of Coastal and Ocean Engineering," Vol. II, J.B. Herbich, ed., Gulf Pub. Co., Houston, TX, Chap. 25.
- Kraus, N.C., and Horikawa, K. (1990). "Nearshore sed. tran.," In "The Sea," Vol. 9,

- Part B, B. Le Mehaute and D.M. Hanes, ed., John Wiley & Sons, Inc. NY, Chap. 22.
- Kraus, N.C., Gingerich, K.J., and Rosati, J.D. (1988). "Towards an improved empirical formula for longshore sand transport," Proc. 21<sup>st</sup> Coastal Eng. Conf., Costa del Sol-Malaga, Spain, ASCE, 1182-1196.
- Leffler, M., Baron, C., Scarborough, B., Hathaway, K., Hodges, P., and Townsend, C. (1998). "Ann. Data Sum. for 1995 CERC FRF," TR CERC-98-14, WES Vicksburg, MS.
- Long, C.E. and Oltman-Shay, J. (1991). "Directional Characteristics of Waves in Shallow Water," TR CERC-91-1, WES Vicksburg, MS.
- Longuet-Higgins, M. S. (1970). "Longshore Currents Generated by Obliquely Incident Sea Waves, I," J. Geophysical Res., Vol. 75, No. 33, 6788-6801.
- Ludwig, K.A., and Hanes, D.M. (1990). "A lab. eval. of optical backscatterance suspended solids sensors exposed to sand-mud mixtures," Mar. Geol., Vol 94, 173-179.
- Schoelhamer, D.H. (1993). "Biological interference of optical backscatterance sensors in Tampa Bay, Florida," Mar. Geol., Vol 110, 303-313.
- Schoonees, J.S., and Theron, A.K. (1993). "Review of the field-data base for longshore sediment transport," Coastal Eng., Vol 19, 1-25.
- Schwartz, R. K., Cooper, D. W., and Etheridge, P. H. (1997). "Sedimentologic Architecture of the Shoreface Prism, Relationship to Profile Dynamics, and Relevance to Engineering Concerns: Duck, North Carolina," TR CHL-97-19, WES, Vicksburg, MS.
- Smith, J. M., Larson, M., and Kraus, N. C. (1993). "Longshore current on a barred beach: field measurements and calculations," J. Geophysical Res., 98(C12), 22,717-22,731.
- Stauble, D.K. (1992). "Long-term profile and sediment morphodynamics: Field Research Facility case history," TR CERC-92-7, WES Vicksburg, MS.
- Sternberg, R.W., Shi, N.C., and Downing, J.P. (1989). "Susp. sed. Meas.," In: Nearshore Sediment Transport, R.J. Seymour, ed., Plenum Press, NY, NY, Chap. 11.
- USACE (1984). "Shore Protection Manual," Vol. I and II, WES, Vicksburg, MS.
- Walton, T. L. (1980). "Computation of Longshore Energy Flux Using LEO Current Observation," CETA 80-3, CERC, WES Vicksburg, MS.
- Watanabe, A. (1991). "Field Application of a Numerical Model of Beach Topography Change," In: Coastal Sediments '91, Ed. by Kraus, et al., ASCE, Seattle, WA.

### Approvals

The author would like to acknowledge the tireless efforts of the STORM team who helped collect these unique data, including: Don Resio, Jarrell Smith, Jane Smith, Ed Hands, Joe Gailani, Dave King, Ernie Smith, Dave Hamilton, Pete Lozis, and others. Permission to publish this paper was granted by the Chief of Engineers.